

Hall effect in iron from 1 to 250 K and to 150 kOe^{†*}

R. W. Klaffky[†] and R. V. Coleman

Department of Physics, University of Virginia, Charlottesville, Virginia 22901

(Received 4 September 1973)

The Hall effect in $\langle 111 \rangle$ iron whiskers with residual resistivity ratios of 3166 and 4000 has been measured in the temperature range 1–247 K. Data for all temperatures in this range have been taken in the field range 15–45 kOe while data at 63.5 and 4.2 K up to 150 kOe have been analyzed. Above 100 K the ordinary Hall coefficient R_0 is linear in both temperature and magnetic field while the ferromagnetic Hall coefficient R_s is nearly proportional to ρ^2 with $R_s = (1.44 \times 10^3/4\pi M_s)\rho^{1.94}$. At temperatures below 80 K the Hall resistivity decreases rapidly with temperature and changes sign from positive to negative at ~ 70 K. It also develops a strong field-dependent curvature below 80 K. This has been taken into account by analyzing Kohler plots of the data over the entire range of temperature and magnetic field. Results suggest that transitions of the carriers from the low-field to the high-field limit may play a critical role in the low-temperature range. Deviations from the Kohler plot are observed between 40 and 20 K and these correspond to an anomalous plateau in the temperature dependence of the Hall resistivity. At 4.2 K the Hall resistivity shows a strong field-dependent curvature up to 100 kOe but is linear in the range 100–150 kOe. Extrapolation of the linear portion to $B=0$ gives a zero intercept indicating that R_s vanishes at helium temperatures. The curvature may result from a mobility transition, but open orbits or magnetic breakdown can also be playing a role. Full discussion of these points is included.

I. INTRODUCTION

In this paper we report the results of measurements of the Hall effect in pure iron whiskers in the temperature range 1–247 K. For most temperatures measurements were made in the field range 0–50 kOe while at 4.2 and 63.5 K the measurements have been extended to 150 kOe. Previous experiments^{1–3} have reported measurements at selected temperatures in the above range, but this is the first time that measurements have been reported for a continuous set of temperatures in this range and in fields up to 150 kOe.

At temperatures above ~ 100 K both the ordinary Hall coefficient R_0 and the ferromagnetic Hall coefficient R_s are smooth functions of temperature and are in essential agreement with previous experiments and theories. Below 100 K the Hall resistivity develops a nonlinear dependence on magnetic field above saturation and this complicates the analysis and separation of the ordinary and ferromagnetic Hall coefficients. The Hall resistivity changes sign from positive to negative as the temperature is reduced below 80 K and this corresponds to a reversal in the sign of the ordinary Hall coefficient R_0 . Separation of the ordinary Hall coefficient R_0 and the ferromagnetic Hall coefficient R_s have been effected by using relations of the form $\rho_H(B) = R_0B + 4\pi M_s R_s$ above 70 K and $\rho_H(B) = R_0B + 4\pi M_s R_s + CB^2$ below 70 K. The coefficients obtained below 70 K using this procedure exhibit several anomalous features and we will examine these in detail.

Examination of Kohler plots of the Hall resistivity over the temperature range below 80 K have

lead us to conclude that some of these anomalous effects may come from a mobility transition corresponding to carriers making the transition from the low-field limit, $\omega_c\tau \ll 1$, to the high-field limit, $\omega_c\tau \gg 1$, as recently suggested by Majumdar and Berger.² Extensive analysis will be given of these effects and the Kohler plots are used to take into account the $\omega_c\tau$ dependence of the Hall resistivity. Data taken at 4.2 K in magnetic fields up to 150 kOe show a linear behavior above 100 kOe and extrapolation of the data above 100 kOe to $B=0$ shows a zero intercept indicating that the ferromagnetic Hall effect approaches zero at 4.2 K. Magnetoresistance measurements have also been made and these will be correlated with the Hall resistivity measurements. Possible open-orbit contributions will also be discussed.

II. EXPERIMENTAL METHODS

Single-crystal iron whiskers grown by the hydrogen reduction^{4,5} of FeCl_2 were used for the experiments. Two $\langle 111 \rangle$ axial whiskers with diameters on the order of 0.5 mm and residual resistivity ratios of 3166 and 4000 were used to measure the Hall voltage and are designated by sample numbers RWK-4 and RWK-5. The Hall leads were spot welded to the $\{110\}$ faces of the crystal and the magnetic field was applied in the $\langle 112 \rangle$ direction for the Hall measurement. The cross section and lead configuration are indicated in the diagram of Fig. 1. The Hall voltage probes were short lengths of nichrome wire which were in turn soldered to copper leads. All leads were thermally grounded to the copper heater block which maintained the sample temperature. Two pairs of Hall leads were

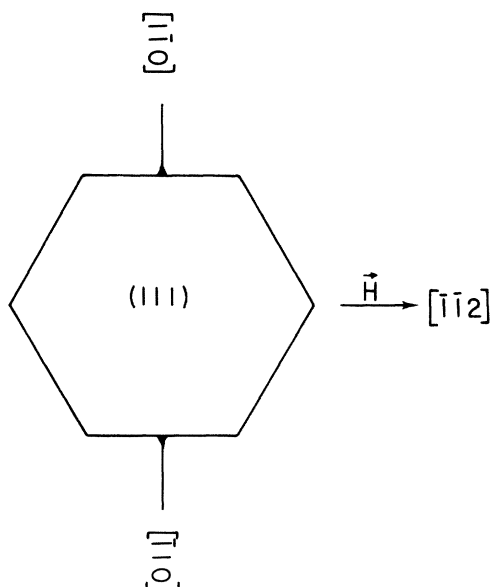


FIG. 1. Lead configuration for Hall-voltage measurement. Hall voltage is measured in the $\langle 110 \rangle$ direction while the field is applied in a $\langle 112 \rangle$ direction. Section of specimen shown is perpendicular to a $\langle 111 \rangle$ direction which is the current direction.

attached to each specimen as a check for reproducibility, one pair near the center of the specimen and one pair nearer to the end. The magnetoresistance leads were spot-welded to the same $\{110\}$ face with a gauge length of 5–10 mm. All thermal voltages were less than $1 \mu\text{V}$ and were essentially independent of temperature indicating that thermal gradients were not a serious problem. The heated copper block provided long-term temperature stability of 0.01 K and was controlled by an Artronix temperature controller using a platinum resistor as a sensor above 40 K while below 40 K a $100\text{-}\Omega \frac{1}{8}\text{-W}$ Allen-Bradley carbon resistor was used as the sensor.

The voltages were recorded using a Keithley 148 nanovoltmeter and source driving a recorder. With the use of careful shielding and grounding techniques, noise levels were reduced to a few nanovolts. For magnetic fields up to 50 kOe a standard helium cryostat and superconducting solenoid system were used with the sample holder mounted in a vacuum can inserted into the solenoid. For fields up to 150 kOe the Bitter solenoids at the Francis Bitter National Magnet Laboratory were used.

The voltage from the transverse Hall pair of leads was measured for positive and negative directions of the magnetic field and for positive and negative current directions corresponding to each field direction. These four values of the voltage were then summed with appropriate signs in order to ex-

tract the transverse odd or Hall voltage, the thermal voltage, and the magnetoresistance plus transverse even voltage. The magnetoresistance term arises from the small misalignment of the transverse contacts which is unavoidable in a transverse two-probe measurement. The transverse even voltage appears to become appreciable only at low temperatures and above 50 kOe so that the magnetoresistance extracted in the above procedure for measurements up to 50 kOe could be compared with the direct magnetoresistance measured in the standard four-lead arrangement. The agreement was good over the whole temperature range and provided a good check on the accuracy of the extraction procedure. Consistency was also good between the two pairs of Hall leads except at a few low-temperature points where the end pair appears to have been influenced by domain effects connected with demagnetization structure near the end of the specimen. The data presented in this paper are always taken from the center pair of leads where variations due to end effects should be minimal.

The low-field points are influenced by multidomain effects and at low temperatures these can produce very large effects in the magnetoresistance as discussed by Shumate *et al.*,⁶ and of course contribute to an averaged Hall voltage rather than that characteristic of a single domain with internal field equal to the saturation magnetization field $4\pi M_s$. Therefore all data points reported here begin above saturation which in these specimens was assured for applied fields above 15 kOe. The magnetic induction was calculated from $B = H + 4\pi M_s - \alpha 4\pi M_s$ where the demagnetizing coefficient α was equal to 0.498 and 0.497 for specimens RWK-4 and RWK-5, respectively.

III. EXPERIMENTAL RESULTS

A. Hall effect

The transverse-odd or Hall voltage is generally given by the following phenomenological equation which expresses the Hall resistance as

$$V_{\text{Hall}}/I = 4\pi M_s R'_s + R'_0 B, \quad (1)$$

or when normalized with respect to the cross-sectional area and distance between leads gives the Hall resistivity

$$\rho_H = E_y/j_x = 4\pi M_s R_s + R_0 B, \quad (2)$$

where R_0 and R_s are the Hall coefficients. The term $4\pi M_s R_s$ is associated with the ferromagnetic Hall effect (also referred to as the anomalous, extraordinary, or spontaneous Hall effect) and is considered to depend only on M_s , the saturation magnetization. The term $R_0 B$ is associated with the ordinary Hall effect and is generally taken to be linearly dependent on B in most experiments.

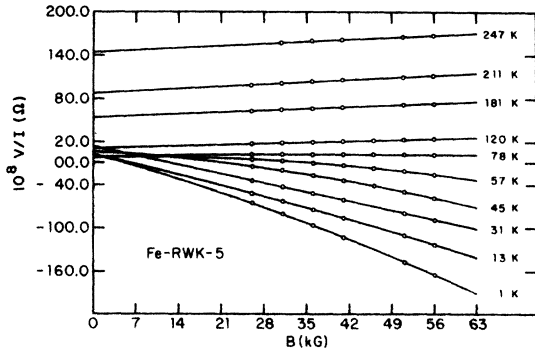


FIG. 2. Plots of the Hall resistance vs magnetic induction for representative temperatures measured in the present experiment. Solid curves drawn through the data points are obtained by a least-squares computer fit to a function of the form $V/I = a + bB + cB^2$. Sample RWK-5 with $RRR = 4000$.

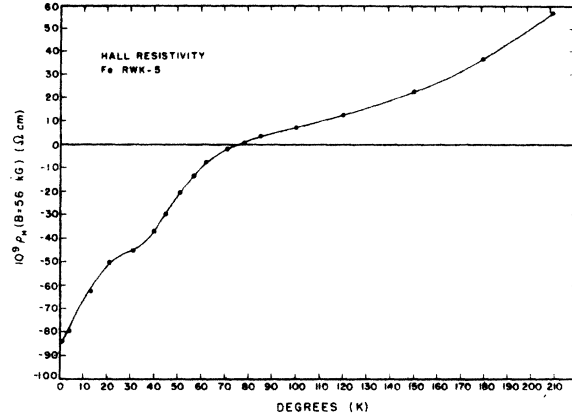


FIG. 4. Hall resistivity ρ_H measured at $B = 56$ kG plotted as a function of temperature in the range 1–210 K. Sample RWK-5 with $RRR = 4000$.

The ordinary Hall effect reflects the balance between electron and hole cyclotron orbits in either the high-field or low-field condition and this bal-

ance may be sensitive to both temperature and field through a dependence on the exact values of $\omega_c \tau$ for the hole and electron orbits, respectively, as well as possible anisotropies in the scattering mechanisms and Fermi surface. These effects can introduce a field dependence greater than linear as well as possible sign changes. In addition, the ferromagnetic Hall effect can possibly exhibit a high-field limit term⁷ proportional to $M_s B^2$. The experimental data definitely show strong nonlinear terms for certain field and temperature ranges and these must be taken into account in any analysis.

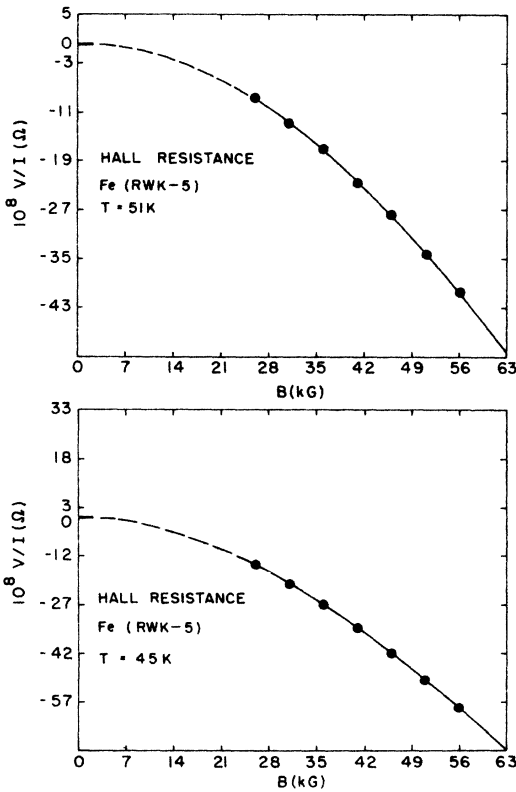


FIG. 3. Hall resistance V/I measured at temperatures of 51 and 45 K where a large nonlinear field dependence is present. Solid curves are drawn from a computer fit of the function $V/I = a + bB + cB^2$. Dashed curves are extrapolations to $B = 0$ using values calculated from Kohler plots (see Fig. 14).

The values of the Hall voltage for magnetic field values well above those required to produce saturation ($H > 15$ kOe, $B > 25$ kOe) have been recorded in the temperature range 1–247 K. Representative curves drawn from a least-squares computer fit of V/I to a function of the form $a + bB + cB^2$ are shown in Fig. 2. A nonlinear dependence on B is clearly evident at high fields for temperatures below 78 K and detailed plots of the data at 51 and 45 K are shown in Fig. 3.

The Hall resistivity ρ_H measured at 56 kG as deduced from the data of Fig. 2 is shown as a function of temperature in Fig. 4. At high temperatures ρ_H is positive and is increasing with increase of temperature due to the ferromagnetic Hall constant which is proportional to the square of the resistivity ρ . Below 85 K, ρ_H begins to decrease rapidly and changes sign from positive to negative between 77 and 72 K for both specimens measured. The decrease in ρ_H continues down to 40 K where a plateau region is observed between 40 and 20 K. Below 20 K, ρ_H continues to decrease attaining a minimum value at the lowest temperature measured, ~1 K. Both specimens show minimum values of ρ_H at 1 K considerably below the value measured by Dheer¹ on his highest-purity specimen and this is consis-

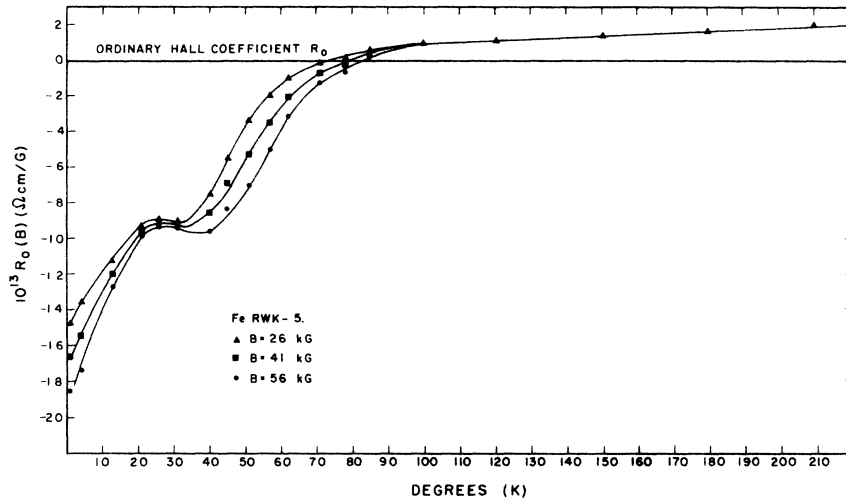


FIG. 5. Derivative of the Hall resistivity with respect to B plotted as a function of temperature. $d\rho_H/dB = R_0(B)$. Above 80 K, $R_0(B) = R_0$ the constant ordinary Hall coefficient. Below 80 K $R_0(B)$ is dependent on magnetic field and is shown for three magnetic fields corresponding to $B = 26, 41, \text{ and } 56 \text{ kG}$.

tent with the fact that his specimen had an RRR equal to about $\frac{1}{10}$ that of the present specimens.

Below 80 K the Hall resistivity develops substantial curvature as a function of magnetic field making separation of the exact coefficients imprecise. However, the curvature can be approximated for purposes of fitting the data by adding a term proportional to B^2 so that the Hall resistivity is given by

$$\rho_H(B) = R_0 B + 4\pi M_s R_s + CB^2. \quad (3)$$

The derivative with respect to the magnetic induction will therefore be given by

$$\frac{d\rho_H}{dB} = 2CB + R_0 = R_0(B). \quad (4)$$

When curvature is not present $d\rho_H/dB = R_0$ as obtained from a conventional linear analysis. In general, $d\rho_H/dB$ will be field dependent and we have designated this by a field-dependent quantity $R_0(B)$. Plots of this quantity as a function of temperature for three different magnetic field values are shown in Fig. 5.

At temperatures above 90 K, $d\rho_H/dB$ is independent of field and equal to R_0 . The value of R_0 increases linearly with temperature above 90 K as observed in previous experiments.^{1,3}

At temperatures below 80 K a field-dependent term is clearly present in $d\rho_H/dB$ and reflects the strong field-dependent curvature present in the Hall resistance. Near 30 K the field dependence nearly vanishes, indicating a return to a linear dependence of the Hall resistance on magnetic field at this temperature. The curvature developing in the Hall resistance as a function of magnetic field below 80 K suggests that a term proportional to $\omega_c \tau$ may be present. The carriers in this range of temperature and field are probably making a transition from the low-field, $\omega_c \tau < 1$, to the high-field, $\omega_c \tau$

> 1 , condition and this transition in turn affects the Hall resistivity. The intermediate maximum in $d\rho_H/dB$ just below 30 K followed by a further strong decrease at lower temperatures indicates that an additional effect possibly associated with scattering mechanisms or with further complexity in the low-field to high-field transition is playing a role.

The traditional computation of the ferromagnetic Hall coefficient would proceed by extrapolation of the Hall resistance curve to $B = 0$ and the value of the intercept obtained would be assigned to a term $4\pi M_s R_s$. For the present data we have carried out such a procedure using both a linear extrapolation, $\rho_H(B) = R_0 B + 4\pi M_s R_s$, and an extrapolation including a term proportional to B^2 , $\rho_H(B) = R_0 B + 4\pi M_s R_s + CB^2$, in a field range up to $B = 56 \text{ kG}$. The resulting values of R_s as a function of temperature are shown in Fig. 6. R_s is positive for all temperatures measured and above 80 K shows a nearly quadratic increase with temperature. The high-temperature values of R_s are in good agreement with the results of Volkenshtein and Fedorov³ for polycrystalline iron and somewhat higher than Dheer's results¹ for $\langle 111 \rangle$ axial iron whiskers.

Below 80 K both the linear and quadratic analyses give an increase in R_s to a relative maximum at 40 K. This anomalous maximum in R_s is a reflection of the variation in the field- and temperature-dependent curvature of the Hall resistivity just below 40 K which also produced the intermediate maximum in $R_0(B)$. In fact, at 31 K the curvature has vanished and the Hall resistivity is a linear function of magnetic field up to 45 kOe (56 kG). Linear extrapolation of the curve at 31 K would give a large nonzero intercept as seen in Fig. 2. Further discussion of the analysis and extrapolation procedure will be given in Sec. IV.

Preliminary data on the Hall effect up to 150 kOe have been obtained for sample RWK-5 at 4.2 and

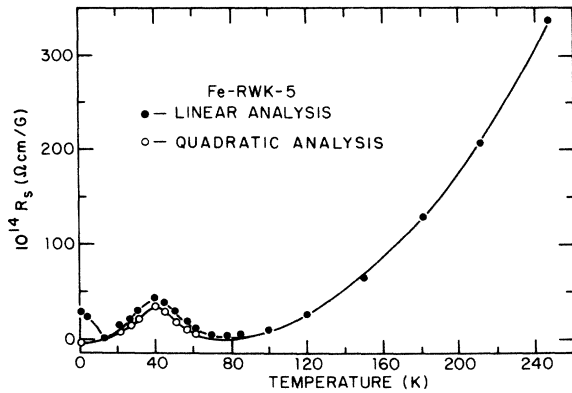


FIG. 6. Ferromagnetic Hall coefficient R_s plotted as a function of temperature in the range 1–247 K. This coefficient is calculated from the intercept of the Hall resistivity obtained by extrapolating to $\bar{B}=0$. Two approximate fits have been used for extrapolation. \bullet : $\rho_H = R_0 B + 4\pi M_s R_s$ (linear analysis); \circ : $\rho_H = R_0 B + 4\pi M_s R_s + C B^2$ (quadratic analysis).

63.5 K. At 4.2 K in the applied field range 20–100 kOe the Hall voltage continues to show a strong non-linear term, but for fields above ~ 100 kOe the Hall voltage shows a linear dependence on magnetic field as shown in Fig. 7. Within the accuracy of the data a straight-line projection of the high-field data back to the origin also gives a zero intercept.

The field dependence of the Hall voltage at 63.5 K has also been measured in applied fields to 150 kOe and results are shown in Fig. 8. In this case the data can be fit by a single B^2 term over the entire field range and this is represented by the solid line. Essentially no linear term is present and this is consistent with the observation that R_0 is very small in this temperature range. The total Hall voltage is also small in this temperature range and

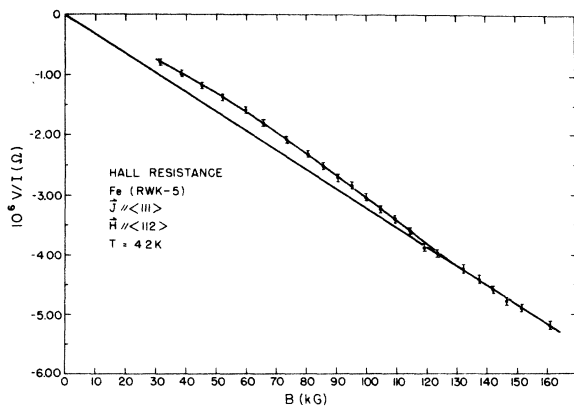


FIG. 7. Hall resistance at 4.2 K plotted as a function of magnetic induction in the range 30–160 kG. Straight solid line passing through the origin represents extrapolation to $B=0$ of the data points above $B=120$ kG.

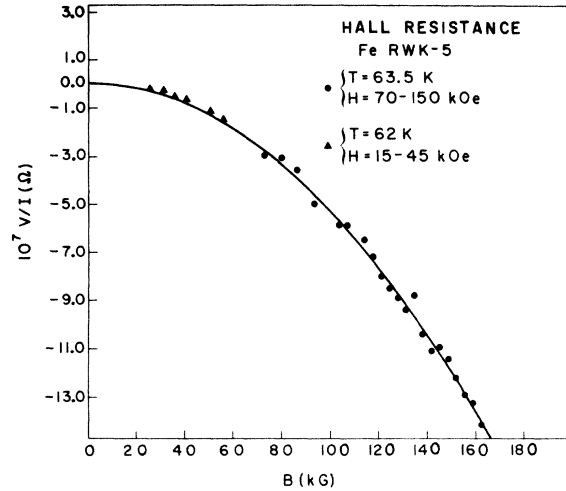


FIG. 8. Hall resistance at 63.5 K plotted as a function of magnetic induction in the range 70–160 kG. Solid curve represents a least-squares computer fit to the data points. Points from 20–60 kG were taken at 62 K. The fit is well represented by a single B^2 term over the entire range.

noise generated when running in the high-field solenoid makes it difficult to measure the small transverse signals below about 50 kOe. In Fig. 8 we have therefore used values for $H < 50$ kOe measured in the superconducting solenoid and have shifted the ordinate of the high-field curve to match the low-field values. This simply means that the values obtained for $H = 50$ –150 kOe are not accurate enough in this temperature range to give a meaningful extrapolated value of the zero-field intercept although a reasonably good estimate of the field dependence at high fields is obtained and this can probably be assigned to the transition in values of $\omega_c \tau$.

B. Magnetoresistance

The magnetoresistance measured for the present specimens at 4.2 K is essentially similar in all respects to the behavior reported from this laboratory in Ref. 9. The transverse magnetoresistance rotation diagram for specimen RWK-5 recorded at $H = 150$ kOe and 4.2 K is shown in Fig. 9. When H is along $\langle 112 \rangle$ the magnetoresistance is described by $\Delta\rho/\rho_0 = aB^n$, where $n \approx 1.8$ for $25 \text{ kG} < B < 100 \text{ kG}$ while for $B > 100 \text{ kG}$, n decreases reaching ~ 1.4 in the range $B \sim 100$ –220 kG as shown in Fig. 10. This behavior suggests that there are weak open-orbit contributions to the magnetoresistance when \bar{H} is in a $\langle 112 \rangle$ direction. However, in the range up to $B = 56$ kG used for most of the Hall-effect data reported in the present paper, the magnetoresistance behavior is essentially that expected for a compensated metal and open orbits have very

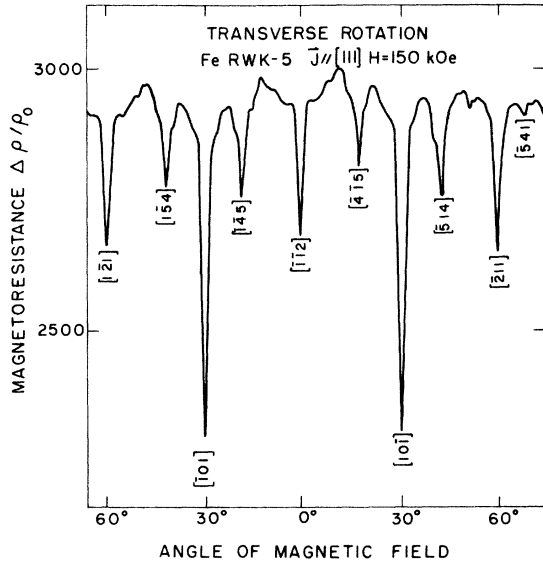


FIG. 9. Transverse magnetoresistance rotation diagram recorded for specimen RWK-5 at 150 kOe. Hall data were taken with field along a $\langle 112 \rangle$ direction which corresponds to a sharp minimum in the magnetoresistance rotation diagram.

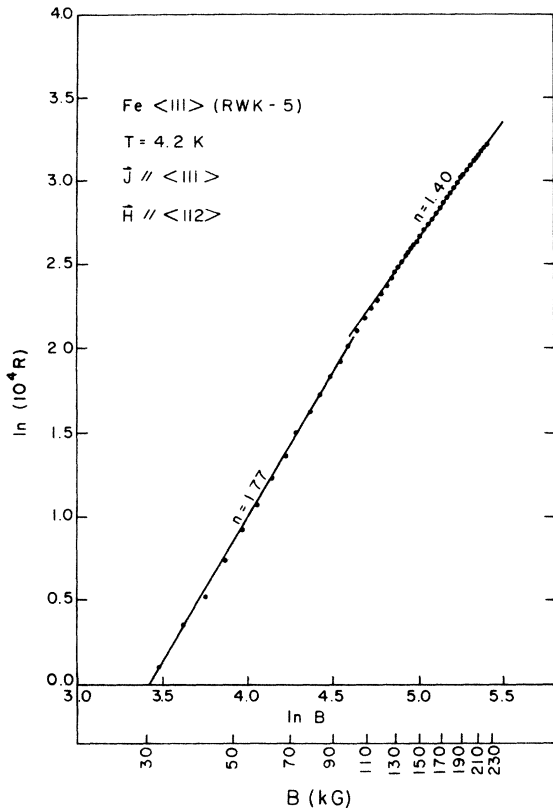


FIG. 10. Log-log plot of the magnetic resistance vs magnetic induction for field in the $\langle 112 \rangle$ direction. Exponent in the relation $R = aB^n$ is indicated for two field regions above and below $B \approx 110$ kG.

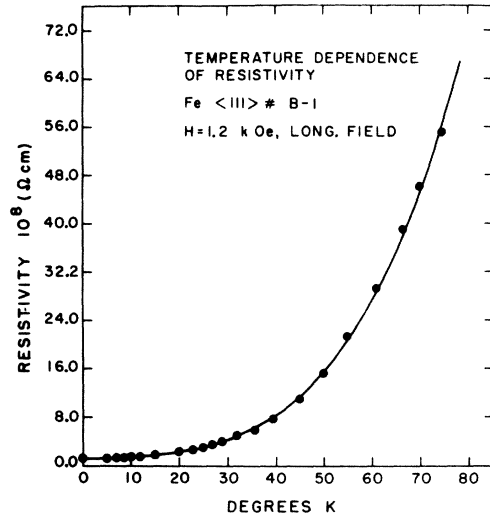


FIG. 11. Resistivity vs temperature for $\langle 111 \rangle$ iron whiskers in the range 0.3–80 K. Data from Ref. 10. Solid curve is a least-squares computer fit to the data points and represents the function $\rho(T) = \rho_0 + 2.4 \times 10^{-11} T^2 + 1.35 \times 10^{-14} T^4$.

little effect. At low temperatures and in magnetic fields above 100 kOe where substantial decreases in the exponent n are observed, open orbits become relatively more important.

The field dependence of resistance up to $B = 56$ kG can be used to make a rough estimate of the $\omega_c \tau$ values characteristic of the specimen used for the Hall-effect measurements. The magnetoresistance in a two-band model of a compensated metal assuming isotropic relaxation times and effective masses can be expressed as

$$\Delta \rho / \rho_0 = C(eB/c)^2 (\tau_e / m_e) (\tau_h / m_h) = C(\omega_c \tau)_e (\omega_c \tau)_h \quad (5)$$

If we further assume equal masses and relaxation times for holes and electrons then $\Delta \rho / \rho_0 = C(\omega_c \tau)_{av}^2$ and we can estimate an average $(\omega_c \tau)_{av}$ over all of the cyclotron orbits by taking $C = 1$ and using experimental values of $\Delta \rho / \rho_0$.

For the highest-purity specimen, RWK-5, the magnetoresistance at 4.2 K and $H \approx 45$ kOe, ($B = 56$ kG) is 480 giving a value of $(\omega_c \tau)_{av} = \sqrt{480} \approx 22$. This would indicate that the average cyclotron orbits satisfy the high-field limit condition, $\omega_c \tau \gg 1$, fairly well for this specimen at 4.2 K in the range 30–56 kG. However, the mobilities in iron clearly vary enormously for various parts of the Fermi surface and a few of the carriers could still be in transition for this field range and temperature.

In order to estimate the values of $\omega_c \tau$ at higher temperatures we can use the temperature dependence of resistance measured for $\langle 111 \rangle$ iron whiskers¹⁰ in the range 1–80 K and shown in Fig. 11. The temperature dependence of resistivity can be

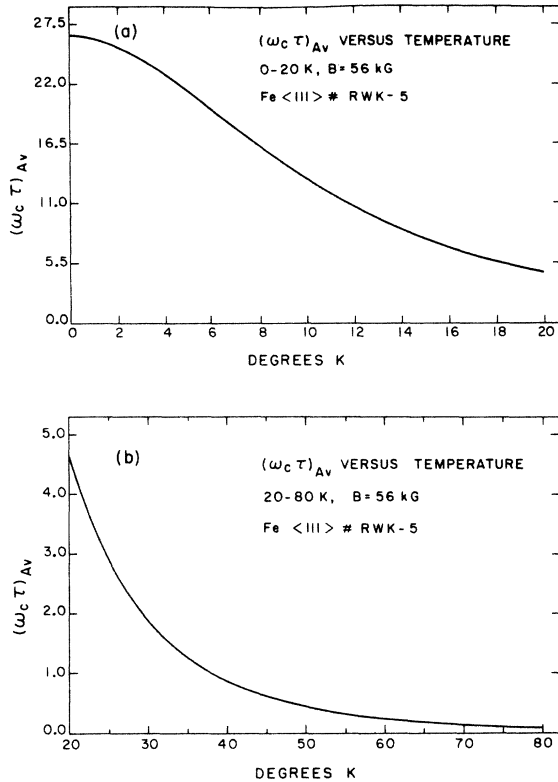


FIG. 12. $(\omega_c \tau)_{av}$ at $B=56$ kG vs temperature for specimen RWK-5 calculated using the function for $\rho(T)$ deduced from the data of Fig. 11. (a) 0–20 K; (b) 20–80 K.

described fairly accurately in the range 0–80 K by the equation

$$\rho(T) = \rho_0 + 2.4 \times 10^{-11} T^2 + 1.35 \times 10^{-14} T^4, \quad (6)$$

which is given by the solid line in Fig. 11. ρ_0 is the residual impurity resistivity and the terms proportional to T^2 and T^4 represent the electron-electron scattering and the electron-phonon scattering, respectively. The T^4 dependence is a much more accurate representation of the electron-phonon scattering than is the more usual T^5 term. This is in agreement with the suggestion that a T^4 dependence may be characteristic of transition metals with strong s - d scattering and intersecting s and d Fermi surfaces.¹¹ If we take the resistance at the longitudinal magnetoresistance minimum as approximately equal to the impurity resistance then for specimen RWK-5 $\rho_0 = 2.0 \times 10^{-9} \Omega \text{ cm}$. In addition, if we take $\rho \sim 1/\tau$ and assume that the temperature dependence of $(\omega_c \tau)_{av}$ depends only on τ then at $B = 56$ kG we have

$$\frac{\rho(4.2 \text{ K})}{\rho(T)} = \frac{(\omega_c \tau)_{av}(T)}{(\omega_c \tau)_{av}(4.2 \text{ K})} = \frac{(\omega_c \tau)_{av}(T)}{22} \quad (7)$$

or

$$(\omega_c \tau)_{av}(T) = 22 \frac{\rho(4.2 \text{ K})}{\rho(T)}. \quad (8)$$

The temperature dependence of $(\omega_c \tau)_{av}$ can therefore be calculated using Eq. (6) for $\rho(T)$ and the result is shown in Fig. 12. The result shows that $(\omega_c \tau)_{av}$ is equal to 1 at ~ 38 K and decreases to 0.1 at ~ 80 K. This implies that mobility arguments based on low-field to high-field transitions can play an increasingly important role in the range below 80 K and must be considered.

The magnetoresistance as a function of temperature at three different fields is shown in Fig. 13. It is clear that below 40 K the magnetoresistance $\Delta\rho/\rho_0$ is becoming large indicating that a substantial number of carriers are making a transition to $\omega_c \tau > 1$. This is also in agreement with the $(\omega_c \tau)_{av}$ value estimated in Fig. 12.

IV. DISCUSSION

The temperature and magnetic field dependences of the Hall effect show a number of features which will require a fairly detailed analysis of all the transport mechanisms which can contribute in a ferromagnetic metal. We will discuss the major mechanisms playing a role in both the ordinary and ferromagnetic Hall effect and attempt to interpret the main features observed in the present experiment.

A. Ordinary Hall effect

The major feature to be explained in the ordinary Hall effect is the change in sign from positive to negative observed as the temperature is decreased in the range near 70 K.

The general interpretation of the ordinary Hall effect is based on a balance between the electronlike and holelike orbits on the Fermi surface. A sign change in the ordinary Hall effect would therefore be associated with a change in the type of orbit

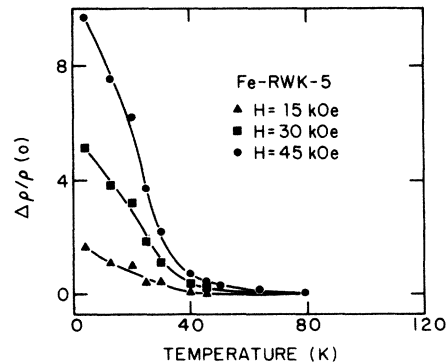


FIG. 13. Magnetoresistance $\Delta\rho/\rho_0$ plotted as a function of temperature below 80 K. Plots show curves for three values of the applied field, $H=15, 30,$ and 45 kOe.

making the dominant contribution to the sum over all orbits. This could occur through a possible change in Fermi-surface topology as a function of temperature, through a change in relative mobility of the hole and electron carriers as a function of temperature, or through strong anisotropies in the Fermi surface and scattering mechanisms which contribute in the various temperature ranges.

The mobilities of holes and electrons can be quite different when carriers in different bands exhibit widely different $\omega_c\tau$ values for a given magnetic field and temperature due to different effective masses or relaxation times. These differences can be expected to play a role when the experimental conditions are such that the specimen makes a transition from the low-field ($\omega_c\tau \ll 1$) to the high-field ($\omega_c\tau \gg 1$) limit over the range of temperature in question or when the basic scattering mechanism changes as a function of temperature. Particular sections of the Fermi surface may also behave locally as electronlike or holelike depending on the value of $\omega_c\tau$. For example, Bragg reflections can come into play as $\omega_c\tau$ increases and these can also change the relative character of the orbits. Further discussion of this general problem can be found in the book by Hurd.¹² The estimates of $(\omega_c\tau)_{av}$ obtained for the specimen RWK-5 give $(\omega_c\tau)_{av} \approx 0.4$ at 50 K and $(\omega_c\tau)_{av} \approx 0.1$ at 80 K when $B = 56$ kG. This estimate would tend to indicate that the sign change in R_0 occurs at temperatures where most of the carriers are still in the low-field limit. However, the estimates of $(\omega_c\tau)_{av}$ are only approximate and the fact that only about 5% of the d electrons are judged to be itinerant¹³ makes it difficult to evaluate the role of mobility precisely. A previous study³ on a much less pure specimen ($RRR = 11.5$) does not show a sign change in R_0 as a function of temperature and suggests that a strong temperature dependence of mean free path must play some role.

Fivaz¹⁴ has explored the idea that the temperature-dependent motion of the Fermi level through a critical crossing point in the band structure could account for the sign change by changing the number of high mobility electrons. Such motion would result from a temperature variation of the ferromagnetic splitting. The accidental degeneracy of the levels Δ_2 and Δ_5 in the spin-up bands of iron would be a good case for the occurrence of such a mechanism. However, most band-structure calculations¹⁵⁻¹⁷ do not place the Δ_2 - Δ_5 crossing at the Fermi level. In addition, recent measurements by Lonzarich and Gold¹⁸ have shown that the temperature-dependent exchange splitting in iron is very small and would not be expected to cause a significant shift of Fermi level.

An alternative explanation for the sign change in R_0 has been developed by Cottam and Stinchcombe¹⁹ based on anisotropy of the Fermi surface and re-

laxation times. They use a two-band model in the low-field limit and introduce parameters to describe the effects of anisotropies in the Fermi surface and relaxation times. In relatively pure specimens they argue that at high temperatures phonon-electron scattering will dominate, at intermediate temperatures Baber or electron-electron scattering²⁰ will dominate, while at the lowest temperatures impurity scattering will dominate. When appropriate values of the anisotropy parameters are used to describe a d band and an s band the model leads to positive values of R_0 at high and low temperatures with negative values at intermediate temperatures in the range below 60 K.

Since the $\omega_c\tau$ values vary widely over the temperature and field ranges used in this experiment it is useful to plot the data in a Kohler plot where the quantities are normalized by dividing by the zero-field resistivity. Measurements at different temperatures on the same sample or on different samples can then be compared on the same curve which essentially represents the normalized quantity as a function of $\omega_c\tau$. Kohler plots for the Hall resistivity are shown in Figs. 14(a)-14(d) for the temperature range 120-4 K. The data generally fall on smooth curves which show a reasonably strong overall curvature down to the lowest temperatures. The data up to 150 kOe at 4.2 K extend the range of $\omega_c\tau$ considerably and these data are plotted on a Kohler plot as shown in Fig. 14(d). For values of B/ρ_0 at 4.2 K corresponding to 100 kOe and above, the Hall resistivity becomes linear and the resulting Kohler plot is of course linear as well. Extrapolation of this linear portion to $B = 0$ gives a zero intercept as shown by the solid line in Fig. 14(d). Data from previous experiments on pure Fe and on an Fe+0.25% Co alloy are also included in Fig. 14.

Deviations from the smooth solid curve are observed in two temperature ranges. At high temperatures above ~ 60 K deviations appear due in part to the larger contribution from the ferromagnetic Hall effect which is proportional to ρ^2 in this temperature range. A deviation is also observed below 40 K where an anomalous plateau in the Hall resistivity and consequent maxima in R_0 and R_s were observed. These deviations are visible in the data for 31, 26, and 21 K plotted near the upper left of Fig. 14(c). The Kohler plot tends to smooth out these deviations, but they are definitely present and account for the S curvature in the Hall resistivity curve of Fig. 4. If this low-temperature deviation is ignored, then the Hall resistivity at temperatures below 80 K is a fairly smooth function of $\omega_c\tau$ and the curvature and sign change below 80 K is likely to be associated with widely different carrier mobilities for the various bands and a transition from the low-field to the high-field limit con-

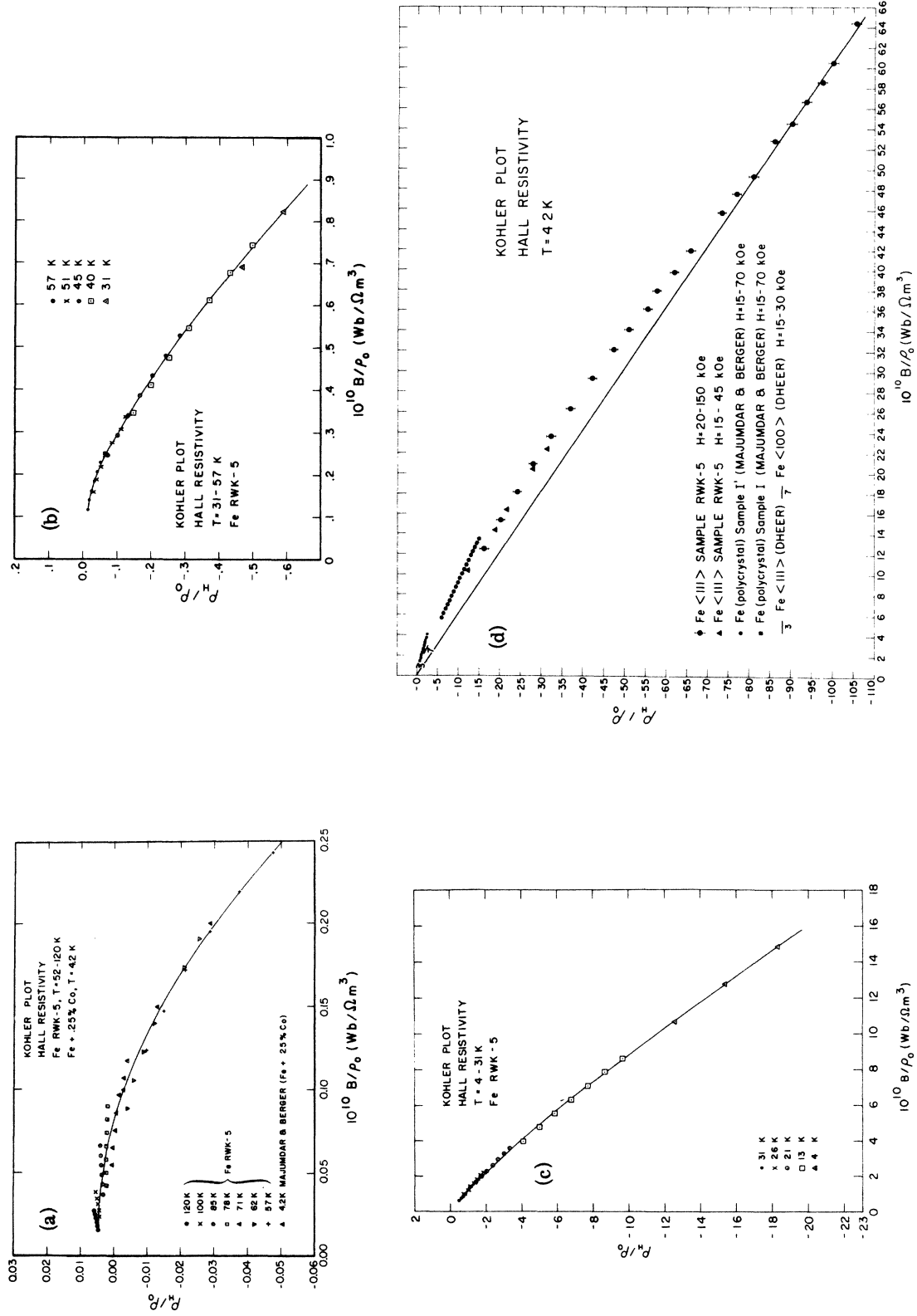


FIG. 14. Kohler plots of the Hall resistivity in the temperature range 4.2–120 K. ρ_H/ρ_0 is plotted as a function of B/ρ_0 where ρ_0 is the resistivity of the sample $H = 0$. (a) Data for sample RWK-5 in the range 57–120 K. Maximum B is 56 kG. (b) Data for sample RWK-5 in the range 31–57 K. Maximum B is 56 kG. (c) Data for sample RWK-5 in the range 4–31 K. Maximum B is 56 kG. (d) Data for sample RWK-5 at 4.2 K. Range of B is 25–161 kG.

dition can occur continuously as the temperature is lowered or the field increased. Majumdar and Berger² have discussed this mobility transition in terms of a four-band model and such a model could be adjusted to fit the smooth curvature observed in the present Kohler plots. As all carriers approach the high-field limit the curvature would be expected to disappear and the Hall resistivity would return to a linear dependence on magnetic field. Such an effect is observed in the data of Fig. 14(d).

The deviation centered on 30 K is at present difficult to explain precisely. At 31 K the Hall voltage shows a linear dependence on field up to 56 kG (see Fig. 2). At lower temperatures it again develops a nonlinear field dependence and this persists down to the lowest temperatures. The temperature range below 40 K corresponds to a range in which the high-field magnetoresistance also becomes large as seen in Fig. 13. This would indicate that below 40 K and at fields above saturation a reasonably large number of carriers are making the transition to the high-field limit condition. The further development of curvature at lower temperatures would then have to be associated with a smaller number of low mobility carriers just entering the low-field to high-field limit transition. In any event there is a rather abrupt change in the process below 40 K and a return of the Hall resistance to a nearly linear dependence on field at 30 K followed by the development of additional nonlinear terms at lower temperatures. This may be due to complexity in the exact details of the mobility transition or it could signal the onset of additional processes affecting the Hall resistivity. Open-orbit contributions may become increasingly important or possible magnetic breakdown effects could contribute as the mean free paths become sufficiently long. Further discussion will be included in Sec. IV C.

B. Ferromagnetic Hall effect

The ferromagnetic Hall coefficient R_H is associated with that part of the transverse voltage which depends on the magnetization of a magnetic metal. Many theoretical papers have been written on the subject and all agree that some aspect of the spin-orbit coupling interaction is responsible for the effect. In the presence of the spin-orbit interaction electrons with spin polarizations parallel and antiparallel to the magnetization are deflected in opposite directions at right angles to the electric current. If the two spin populations are unequal then a net transverse current appears which is cancelled by the resulting Hall voltage.

In the original work of Karplus and Luttinger²¹ the transverse current was associated with the force due to the spin-orbit part of the periodic potential and gave rise to a nonvanishing effect only if the carriers in a given band were coupled to other

bands through the spin-orbit interaction. Strachan and Murray²² made a somewhat more complete calculation of these effects using conventional quantum-mechanical transport theory to consider the motion of the electrons under the influence of electric field components and spin-orbit coupling allowing for all possible intraband and interband effects. Subsequent treatments of the problem have been carried out by Smit,²³ Kondo,²⁴ and Maranzana²⁵ in which the spin-orbit part of the perturbing potential of the scattering center as well as the central periodic part has been considered. This analysis results in a skew or asymmetric scattering of the electrons and gives a nonvanishing result with the required symmetry only when the scattering probability is calculated in the second Born approximation. In general, calculations of skew scattering in the second Born approximation using plane waves as unperturbed wave functions give results which are much too small to explain the magnitude of the experimental results.

Leroux-Hugon and Ghazali²⁶ have reconsidered the skew scattering by using wave functions which properly include the periodic part of the spin-orbit interaction and when calculated in the second Born approximation the transition probability leads to a transverse resistivity in the Hall geometry which they estimate to be of the right order of magnitude to agree with experiment. The influence of the periodic part of the spin-orbit interaction on the skew scattering has also been considered in a theory by Fivaz.²⁷

In addition to the contributions considered in the above theories Berger²⁸ has recently considered nonclassical terms in the Boltzmann equation which become important for very short mean free paths corresponding to conditions where the parameter $\hbar/\epsilon_F\tau$ is appreciable. ϵ_F is the Fermi energy and τ is the relaxation time of the electrons. These terms probably become important at high temperatures or in concentrated alloys. When calculated in the presence of spin-orbit coupling these terms result in a side-jump displacement at every scattering of the electron on impurities or phonons. This displacement is on the order of 10^{-11} m and results because the impurity or phonon distorts the wave function locally and creates a local current density. For short mean free paths and a random distribution of impurities or phonons, interference phenomena can be neglected and the first-order Born approximation is sufficient to obtain a contribution to the ferromagnetic Hall resistivity of the right order of magnitude.

In high-purity metals at reasonably high temperatures, the electron scattering is dominated by the electron-phonon interaction and Leribaux²⁹ was the first to calculate the ferromagnetic Hall coefficient specifically in the electron-phonon interac-

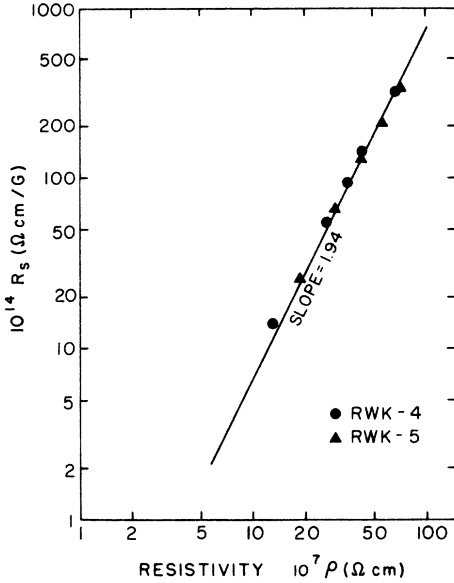


FIG. 15. Log-log plot of the ferromagnetic Hall coefficient R_s as a function of resistivity. Temperature range for data points is 80–247 K.

tion regime. Leribaux used Kubo's formal solution of the transport problem³⁰ to calculate the antisymmetric component of the ferromagnetic Hall conductivity tensor and derived an expression for the transverse conductivity tensor that resulted from a term of zero order in the electron-phonon interaction. The results have been specifically applied to iron by evaluating matrix elements of the spin-orbit operator between wave functions constructed to properly represent Wood's³¹ dispersion curves for iron. The main contributions came from bands close to the Fermi surface and using symmetry arguments Leribaux suggested that the major contribution results from the spin-up band that is nearly spherical about the Γ point. Leribaux's expression for the ferromagnetic Hall coefficient is

$$R_s = \frac{20.9}{4\pi M_s(T)} \rho_{xx}^2 (1 + 1.12 \times 10^{-8} T^2) \frac{\Omega \text{ cm}}{\text{G}}. \quad (9)$$

This essentially assigns all of the temperature dependence to ρ_{xx}^2 as was also a consequence of the original Karplus and Luttinger theory where the inversion of the conductivity tensor automatically results in a Hall resistivity proportional to the resistivity squared.

Berger's theory of the side-jump mechanism also leads to a dependence of R_s on ρ^2 and his expression based on an estimated value of the effective spin-orbit enhancement factor is

$$R_s = (\sigma_{xy}/4\pi M_s) \rho^2 = (10^2/4\pi M_s) \rho^2 \Omega \text{ cm/G}. \quad (10)$$

The proportionality factor is therefore approximately a factor of 5 greater than that derived in Leribaux's theory.

In the present experiment the high-temperature data in the range 100–247 K obey an expression of the form

$$R_s = (1.44 \times 10^3 / 4\pi M_s) \rho^{1.94}, \quad (11)$$

where R_s is in $\Omega \text{ cm/G}$, M_s in G and ρ in $\Omega \text{ cm}$ as indicated in the plot of Fig. 15.

The expected dependence on ρ^2 is clearly confirmed, but the constant of proportionality is larger than estimated in either theory. However, the estimates made in the theories are probably only valid to within an order of magnitude and the present results are not unreasonable with respect to such estimates. Our result is essentially in agreement with that of Dheer¹ who found a somewhat lower coefficient of proportionality, his average value being equal to $9.3 \times 10^2 / 4\pi M_s$.

Below 100 K the values of R_s are difficult to extract precisely due to the field-dependent curvature developing in the Hall resistivity. By using either a linear or quadratic extrapolation as previously shown in Fig. 6 an anomalous maximum near 40 K is observed for R_s . In the linear extrapolation an anomalously high value of R_s is also observed at 4 K and below as was previously reported by Dheer.¹ The 4-K anomaly is clearly a result of the curvature and is removed in a quadratic analysis or in an extrapolation using only data for B greater than 100 kG at 4.2 K.

The anomalous maximum at 40 K is a reflection of the deviation from a smooth Kohler plot in this region and cannot be easily removed unless one ignores the vanishing of the curvature at 31 K and approximates the behavior with a smooth Kohler plot with continuous downward curvature over this region. In this case one can use the smooth Kohler plots to extrapolate values of ρ_H/ρ_0 for values of B/ρ_0 below saturation at a given temperature. This procedure is used to extrapolate the curves (dotted lines) in Fig. 3 at 51 and 45 K and intercepts close to zero are obtained indicating that in this approximation R_s is decreasing monotonically with temperature. It should be emphasized, however, that the experimental data give a subtle deviation from the Kohler plot below 40 K and this is reflected in an anomalous region for both R_0 and R_s . Whether there is a true contribution to R_s or whether this represents a complex transition in the normal transport process is difficult to decide at present.

C. Open orbits and magnetic breakdown

At low temperatures and values of $\omega_c \tau > 1$ we must also consider the possible effects of open orbits or slight discompensation. Magnetic breakdown effects can also influence the Hall resistivity

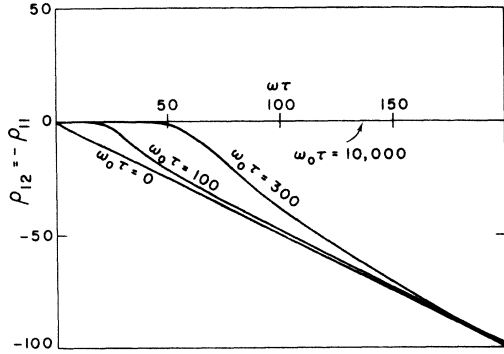


FIG. 16. Hall resistance due to magnetic breakdown from closed compensated orbits to open and closed (hole) orbits. $\omega_0\tau$ represents $\omega_c\tau$ value corresponding to breakdown field H_0 .

and these cannot be ruled out as yet. As previously mentioned, the field direction used in this experiment corresponds to a weak open-orbit minimum in the magnetoresistance rotation diagram and this is reflected in a decreasing value of the exponent n in $\Delta\rho/\rho_0 = B^n$ for applied field above 100 kOe at 4.2 K. Fawcett and Reed⁸ have given a simplified version of the resistivity tensor describing the effects of open orbits or discompensation and the Hall resistivity term is given by

$$\lim_{\gamma \rightarrow 0} \frac{\rho_{xy}}{\rho_0} = \frac{(D+N)\gamma + \gamma^2}{D\gamma^2 + (D+N)^2\gamma^2 + \gamma^4}, \quad (12)$$

where $\gamma = 1/(\langle\omega_c\tau\rangle_{av})$, $N = (|n_e - n_h|)/(n_e + n_h)$, n_e and n_h being the number of electrons and holes per unit cell, respectively, and D is the fraction of open orbits. For either $D \neq 0$ or $N \neq 0$ and $D/\gamma^2 \gg 1$ or $N^2/\gamma^2 \gg 1$, the Hall resistivity ρ_{xy} is linear in B . At lower fields where D/γ^2 or N^2/γ^2 are not very large compared to 1, terms proportional to B^2 and B^3 will be observed. This could account for the curvature in Figs. 7 and 14(d), although a comparison to the magnetoresistance behavior at 4.2 K in the same field range raises some question. The transverse magnetoresistance described by the same resistivity tensor gives for $D \neq 0$ and $N = 0$

$$\frac{\rho_{yy}}{\rho_0} = \frac{1}{D + \gamma^2} = \frac{t^2}{1 + Dt^2} \quad (13)$$

or for $N \neq 0$ and $D = 0$

$$\frac{\rho_{xy}}{\rho_0} = \frac{\rho_{xy}}{\rho_0} = \frac{2}{N^2\gamma^2 + \gamma^4} = \frac{t^2}{1 + N^2t^2}, \quad (14)$$

where $t = 1/\gamma = (\omega_c\tau)_{av}$.

These expressions predict a deviation from quadratic field dependence and eventual saturation of the magnetoresistance in a compensated metal if open orbits or discompensation are present. We observe a substantial decrease from quadratic behavior at high fields as shown in Fig. 10, but com-

plete saturation has not been reached and this would be inconsistent with the observed linear dependence of the Hall effect which should occur in the same limit as saturation of the magnetoresistance if this were a complete description of the effects. Further experiments at high fields may resolve this point.

Iron has sufficiently complex Fermi surface^{32,33} that a number of possibilities exist for magnetic breakdown between various sections of either the majority or minority spin Fermi surface. If, in addition, possible spin hybridization is taken into account then additional breakdown points can exist where dehybridization of the orbit would occur above the breakdown field. In either case various orbits would be coupled through magnetic breakdown and the resultant change in topology can have major effects on both the high-field magnetoresistance and Hall resistivity.

Falicov and Sievert³⁴ have considered a range of cases including most of those that are of physical interest regarding changes in the connectivity of orbits. The original paper should be consulted for details, but the specific case for transitions from closed compensated orbits to open and closed (hole) orbits has been calculated and the behavior of the Hall resistivity as a function of $\omega_c\tau$ is shown in Fig. 16. The breakdown probability is given by $P = e^{-H_0/H}$ where the breakdown field $H_0 = K\Delta^2 Mc/E_f eh$; Δ is the energy gap between the bands involved. In Fig. 16 the breakdown field H_0 is represented by the equivalent $\omega_0\tau$ value and curves are shown for three representative values of $\omega_0\tau$. It is clear that such curves could reproduce the behavior observed in the high-field Hall resistivity plotted in Fig. 14 for fields up to 150 kOe at 4.2 K. Further experiments at higher fields will be necessary to evaluate this possibility in detail.

V. CONCLUSIONS

Measurements of the Hall effect in high-purity iron whiskers in the temperature range 1–250 K have revealed a rather complex behavior over this temperature range and several mechanisms will probably be required to explain all of the features in detail. One of the prominent features is a change in sign of the Hall resistivity from positive to negative as the temperature is decreased below 80 K. This is due to a change in sign of the ordinary Hall coefficient R_0 which is a rapidly decreasing function of temperature below 80 K except for a plateau near 30 K. Above 100 K, R_0 increases linearly with temperature and is in essential agreement with previous measurements of the Hall effect in iron. Above 100 K, R_s is described by the relation $R_s = (1.44 \times 10^3/4\pi M_s)\rho^{1.94}$ in general agreement with previous experimental and theoretical results which give $R_s \sim \rho^2$.

Below 80 K the Hall resistivity develops a strong

nonlinear dependence on magnetic field giving rise to strong downward curvature in the Hall voltage as a function of magnetic field. This curvature makes separation of the ordinary and ferromagnetic Hall coefficients fairly complex. If the coefficients are extracted using an expression $\rho_H(B) = R_0 B + 4\pi M_s R_s + CB^2$ to fit the data then R_s shows an anomalous maximum near 40 K and R_0 shows a plateau near 30 K.

The overall curvature of the Hall resistivity appears to be connected with a mobility transition due to carriers which make a transition from the low-field to the high-field limit condition as temperature is reduced or magnetic field increased. This dependence on $\omega_c \tau$ has been examined by making Kohler plots of the Hall resistivity over the whole range of temperature and magnetic field.

Deviations from the smooth Kohler plot are observed at high temperatures where the ferromagnetic Hall effect begins to make major contributions and in the range below 40 K where the Hall resistivity shows an S curvature as a function of temperature. This reflects the onset of a sudden change in scattering mechanism or an additional complexity in the mobility transition. This anomaly also shows up in the vanishing of the nonlinear field term at 31 K and its reappearance at lower temperatures.

At 4.2 K Hall resistivity measurements have been made up to 150 kOe and nonlinear field dependence is observed up to 100 kOe followed by a linear field dependence at higher fields. Extrapolation of the high-field data to $B = 0$ gives a zero intercept indicating that R_s has decreased to nearly zero at 4.2 K. This behavior would be consistent with a mobility transition as discussed by Majumdar and Berger² in which the Hall resistivity shows a linear field dependence only after all carriers have reached the high-field limit condition. On the other hand, open orbits or magnetic breakdown could also be producing a similar behavior in the low-temperature range and further experiments will be necessary in order to develop a complete understanding of the effects.

ACKNOWLEDGMENTS

The authors would like to acknowledge Professor L. M. Falicov and Professor D. J. Sellmyer for many stimulating discussions. Professor R. C. Morris has contributed extensively to carrying out many aspects of the experiments. We also would like to thank Dr. J. G. Beitchman for use of his unpublished data. Larry Rubin and his group have contributed to the work at the National Magnet Laboratory.

*Work supported by U. S. Atomic Energy Commission Contract No. At-(40-1)-3105.

†Work above 80 kOe was performed while the authors were Guest Scientists at the Francis Bitter National Magnet Laboratory, which is supported by the National Science Foundation.

‡Present address: Physics Department, University of Connecticut, Storrs, Connecticut 06268.

¹P. N. Dheer, Phys. Rev. **156**, 637 (1967).

²A. K. Majumdar and L. Berger, Phys. Rev. B **7**, 4203 (1973).

³N. V. Volkenshtein and G. V. Fedorov, Zh. Eksp. Teor. Fiz. **38**, 64 (1960) [Sov. Phys.-JETP **11**, 48 (1960)].

⁴R. V. Coleman, Metall. Rev. **9**, 261 (1964).

⁵S. S. Brenner, *The Art and Science of Growing Crystals*, edited by J. J. Gilman (Wiley, New York, 1963), Chap. 2, p. 30.

⁶P. W. Shumate, Jr., R. V. Coleman, and R. C. Fivaz, Phys. Rev. B **1**, 394 (1970).

⁷L. Berger, Phys. Rev. **177**, 790 (1969).

⁸E. Fawcett and W. A. Reed, Phys. Rev. **134**, A 723 (1964).

⁹R. V. Coleman, R. C. Morris, and D. J. Sellmyer, Phys. Rev. B **8**, 317 (1973).

¹⁰J. G. Beitchman, C. W. Truseel, and R. V. Coleman, Phys. Rev. Lett. **25**, 1291 (1970); J. G. Beitchman, Ph.D. thesis (University of Virginia, 1970) (unpublished).

¹¹J. M. Ziman, *Electrons and Phonons* (Oxford U. P., London, 1960), p. 378.

¹²Colin M. Hurd, *The Hall Effect in Metals and Alloys*

(Plenum, New York, 1972).

¹³M. B. Stearns, Phys. Rev. B **8**, 4383 (1973).

¹⁴R. C. Fivaz, J. Appl. Phys. **39**, 1278 (1968).

¹⁵S. Wakoh and J. Yamashita, J. Phys. Soc. Jap. **21**, 1712 (1966).

¹⁶K. J. Duff and T. P. Das, Phys. Rev. B **1**, 192 (1971).

¹⁷R. A. Tawil and J. Callaway, Phys. Rev. B **7**, 4242 (1973).

¹⁸G. Lonzarich and A. V. Gold, Can. J. Phys. **52**, 694 (1974).

¹⁹M. G. Cottam and R. B. Stinchcombe, J. Phys. C **1**, 1052 (1968).

²⁰N. F. Mott, Adv. Phys. **13**, 325 (1964).

²¹R. Karplus and J. M. Luttinger, Phys. Rev. **95**, 1154 (1954).

²²C. Strachan and A. M. Murray, Proc. Phys. Soc. **73**, 433 (1959).

²³J. Smit, Physica **24**, 39 (1958).

²⁴J. Kondo, Prog. Theor. Phys. **27**, 772 (1962).

²⁵F. E. Maranzana, Phys. Rev. **160**, 421 (1967).

²⁶P. Leroux-Hugon and A. Ghazali, J. Phys. C **5**, 1072 (1972).

²⁷R. C. Fivaz, Phys. Rev. **183**, 586 (1969).

²⁸L. Berger, Phys. Rev. B **2**, 4559 (1970).

²⁹H. R. Leribaux, Phys. Rev. **150**, 384 (1966).

³⁰R. Kubo, J. Phys. Soc. Jap. **12**, 510 (1967).

³¹J. H. Wood, Phys. Rev. **126**, 517 (1962).

³²A. V. Gold, L. Hodges, P. T. Panousis, and D. R. Stone, Int. J. Magn. **2**, 357 (1971).

³³David R. Baraff, Phys. Rev. B **8**, 3439 (1973).

³⁴L. M. Falicov and Paul R. Sievert, Phys. Rev. **138**, A88 (1965).